DESIGN AND ANALYSIS OF AN INNOVATIVE CUBESAT THERMAL CONTROL SYSTEM FOR BIOLOGICAL EXPERIMENT IN LUNAR ENVIRONMENT

IAC-18-F1.2.3

DESIGN AND ANALYSIS OF AN INNOVATIVE CUBESAT THERMAL CONTROL SYSTEM FOR BIOLOGICAL EXPERIMENT IN LUNAR ENVIRONMENT

C. Conigliaro [a], D. Calvi[b], L. Franchi[c], F. Stesina[d], S. Corpino[e]

[a] *Department of Energy, Politecnico di Torino, Corso Duca degli Abruzzi, 10129 Torino, Italy*, christian.conigliaro@polito.it
[b] *Department of Mechanical and Aerospace Engineering, Politecnico di Torino, Corso Duca degli Abruzzi, 10129 Torino, Italy*, daniele.calvi@polito.it
[c] *Department of Mechanical and Aerospace Engineering, Politecnico di Torino, Corso Duca degli Abruzzi, 10129 Torino, Italy*, loris.franchi@polito.it
[d] *Department of Mechanical and Aerospace Engineering, Politecnico di Torino, Corso Duca degli Abruzzi, 10129 Torino, Italy*, fabrizio.stesina@polito.it
[e] *Department of Mechanical and Aerospace Engineering, Politecnico di Torino, Corso Duca degli Abruzzi, 10129 Torino, Italy*, sabrina.corpino@polito.it

Abstract

After about 50 years since the Apollo missions, Space Agencies are planning new manned missions beyond LEO, aiming to full functional Lunar and Martian outposts. Leaving the protection of Earth's magnetic field, human body will be exposed by a huge amount of harmful radiations coming from both solar wind and cosmic rays, which represent a risk for the astronauts. In order to prepare for future manned exploration missions, many biological experiments have been conducted inside and outside the International Space Station (ISS). From these experiments, engineers and scientists gained knowledge about biological degradation after a long period of exposure to space radiations. Similar experiments were also carried out in small free-flyers. For example, the O/OREOS mission is built with a 3U CubeSat that is evaluating how microorganisms can survive and can adapt to the harsh orbit environment. Small platforms, such as CubeSats, are gaining interest for many applications including science experiments. Biological payloads require very stable environmental conditions, implying that environment requirements are very stringent and that existing passive thermal control systems may not be sufficient to support these class of experiments. The goal of this paper is to describe and discuss the design of an active environmental control system suitable for supporting biological payloads hosted onboard nanosatellites. In particular, we focused the attention on the case of a payload constituted by a bacterial culture that needs oxygen supply for growing up. The rate of growth and vitality are measured through bacteria metabolic parameters. The reference mission is built with a 6U CubeSat in Lunar Polar Orbit, with the main scientific objective of measuring the effect of the lunar radiation environment on a culture of "Bacterium Deinococcus Radiodurans". This kind of bacteria exhibits significant resistance to ionising radiation and the survival temperature range is 30°C ± 10°C. The thermal control system (TCS) is constituted by Stirling cryocooler, Peltier cells and heaters. The aforementioned pieces of equipment operate on the oxygen tank and test chamber in order to control temperature of the oxygen necessary for the growth of the bacteria. To verify the temperature requirements, two kinds of analysis are performed: radiative analysis, to have information about the heat fluxes from space environment; and lastly, a thermo-fluid dynamics analysis, to gather data about temperature in the test chamber. As result, it is possible to confirm that, with the chosen TCS, the temperature requirement is verified during the mission.

Keywords: TCS, SmallSat, CubeSat, Moon, Thermal Analysis, Biological payload

Nomenclature

ρ	Density	α	Absorptivity
C_p	Specific heat	ε	Emissivity
K	Conductivity coefficient	a	Albedo coefficient
T	Temperature	C_{IR}	IR planet coefficient
Q	Heat energy	F_{ij}	view factor from surface i and surface j
t	Time	σ	Stephan-Bolzman constant
q_s	Heat flux (Solar direct)		
q_A	Heat flux (Albedo)	p	Pressure
q_{IR}	Heat flux (IR planet)	τ	viscous stress tensor
S	Solar constant	h	Specific enthalpy
F_p	Planet view factor	u	Flow speed vector

Re	Reynolds number

Acronyms/Abbreviations

CRaTER	Cosmic Ray Telescope for the Effects of Radiation
HW	Hardware
IR	Infra-Red
LRO	Lunar Reconnaissance Orbit
RAAN	Right Ascension of the Ascending Node
SNR	Signal-to-Noise Ratio
TCS	Thermal Control System
TEC	Thermo-Electric Coolers
TRL	Technology Readiness Level

1. Introduction

According to the Global Exploration Roadmap [1], the interest of the space agencies is to pursue the objective of expanding the human presence into the Solar System, targeting to Moon and Mars as future destinations.

In order to achieve the return of mankind on the lunar surface, it is needed to fill some gaps in knowledge. One of the main topics is the cosmic radiation that is considered the main health hazard for manned exploration and colonization of the Solar System [2]. Despite the numerous measurement around the Earth and in deep space, the only data available for the lunar environment are limited to the ones from the CRaTER experiment within the mission Lunar Reconnaissance Orbiter (LRO) [3] and from the Indian Chandrayaan-1 mission [4].

To this purpose, a fast-delivery and low-cost satellite mission could increase the number of radiation measurements thus filling the gaps of knowledge of this field of research. The advent of micro- and nano-satellites represents a disruptive technology that might change the way we approach space exploration. Many education-driven and technology demonstration missions have already been flown (some information about these missions are reported in the references [5] [6] [7] [8]), but it is a fact that they have gained popularity far beyond university labs. Many agencies have fostered this interest for smallsats, such as CubeSats, expanding the potential of the space missions they can accomplish, especially for science and exploration applications.

In addition, in the last few years, this type of spacecraft has been pushed towards a new direction: interplanetary missions. Numerous examples of mission concepts for interplanetary CubeSats have been presented ([9], [10], [11]), ranging from lunar missions (such as LunaH-Map, Lunar IceCube [12]) to Mars missions (MarCO [13]) and asteroid missions (NEAScout [14]).

In order to achieve the objectives of these kind of missions, a few critical technical areas need to be addressed, among which propulsion, thermal, navigation, and communications.

Among them, the Thermal Management System (TMS) is a challenging area of research ([15]), especially for missions with stringent thermal requirements such as astrobiology experiments, or spectral bands observation (e.g. InfraRed imaging payloads). Thus, a passive Thermal Control System (TCS) cannot keep an adequate range of operative temperature in a harsh environment such as the deep space.

Typical active thermal devices include electrical resistance heater and coolers but the use of this kind of TCS is limited. Nowadays, the heater is used to maintain the operative temperature for the battery in addition to passive TCS. Furthermore, heaters have often been used to control the temperature of a biological payload (GeneSat, PharmaSat, O/REOS, SporeSat, EcAMSat and Biosentinel) [16].

To decrease the temperature, it is possible to use coolers and cryocoolers that have been a recent improvement for smallsat technologies [16]. This type of TCS is useful for that components that require a low temperature in order to have high performance, such as IR sensor. Among the coolers, there are the Thermo-Electric Coolers (TEC) or Peltier Cells, used in Earth observation mission, such as CanX-2 [17].

However, systems to reach cryogenic temperature have a maximum Technology Readiness Level (TRL) of 7. Indeed, Cryocube-1 will be the first CubeSat mission that will perform cryogenic management test on orbit in 2018 [18] within the NASA ELaNa programme.

The study presented in this paper investigates the feasibility and the design of a TMS for biological payload in a lunar 6U CubeSat mission.

The study focuses on the thermal analysis of the payload, for which a radiative analysis and thermo fluid-dynamic analysis has been performed. In addition, active TCSs are considered in order to enhance the technological capabilities with respect to current state-of-the-art technology.

2. Reference Mission

2.1 MoonCARE

The MoonCARE project is a CubeSat mission, developed by VKI, DLR, Tyvak International and Politecnico di Torino during the ESA LUCE Phase A study [19]. The maximum mission lifetime is 2 years and the following science goal shall be achieved:

1. Science Goal: To understand the unique lunar radiation environment and its dependency on solar activity and seasonal variation

• Objective: To characterise the radiation environment in the vicinity of the Moon with unprecedented spatial and temporal resolution

2. Science Goal: To understand how the lunar radiation environment affect the proliferation of a specific organism

• Objective: To study the survival and active metabolism in the extreme lunar radiation environment.

In order to achieve these objectives, after the first design iteration, a space segment composed by three 6U Cubesat have been designed with two payloads for radiation environment measurement and astrobiology experiment.

The reference orbit is a Lunar Polar Orbit and the orbital parameters in the Table 1 are reported:

Table 1: orbital parameter [2]

Inclination [deg]	90
Periselenium [km]	150
Aposelenium [km]	600
Cubesat true anomaly spread [deg]	45
Period [min]	145

The configuration of the Spacecraft is reported in the following figure (Fig. 1):

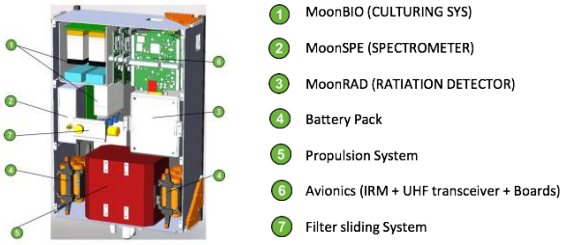

Fig. 1. MoonCARE spacecraft configuration [19]

For the payload used for astrobiology experiment (MoonBIO), the hardware (HW) provides culturing conditions and supports the metabolism of the microorganisms that are exposed to the Moon radiation climate. Survival and proliferation rate of the organisms will be automatically measured in situ as an increase in absorbance with time. Comparison of the results with more shielded cultures allows the determination of the radiation effect. During the experiment, considering a culture of "Bacterium Deinococcus Radiodurans", a controlled temperature of 30 °C ± 10 °C is required ().

The payload considered in this study has a volume of 1U and it bases on SESLO module of O/OREOS mission [20].

Fig. 2. SESLO module [20]

The remaining 1U is dedicated to the Absorbance measurement unit with a spectrometer instrument (MoonSPE) for in situ monitoring of growth of biological cultures via optical absorbance measurements at 490 or 600 nm ± 10 nm, 2 times per day.[2]

The detail of the test chamber payload is reported in the following figure:

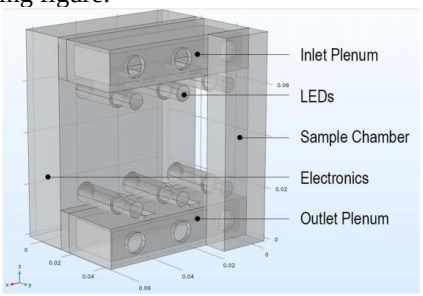

Fig. 3: MoonBIO test chamber. The dimension are measured in [m]

The test chamber is the item where the microorganisms must live and kept under observation. In particular, the bacterial cultures lie in the sample chamber (Fig. 4) while the oxygen flow, that supplies the organisms, enters inside the chamber from the *inlet hole* and it comes out through the *outlet hole*. A breathable membrane provides the oxygen supply.

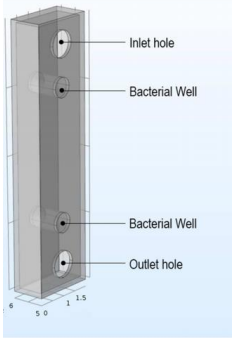

Fig. 4: Sample chamber. The dimensions are measured in [m]

To guarantee the close-loop circuit, the inlet and outlet holes are linked by a pipe-line and the airflow is

moved thanks to a fan (Fig. 5). The material used for the entire test chamber is PEEK.

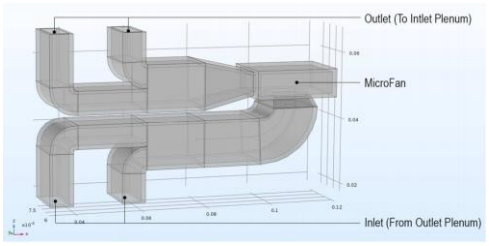

Fig. 5: Pipe-line. The dimensions are measured in [m]

As it has been mentioned before, the organism consumes oxygen in order to grown up. Thus, the oxygen supply is guarantee thanks to a tank of 0.032 L.

The material of the tank is Aluminium and surface finishes of 2 mil Aluninized Kapton is considered in order to reduce the emittance from 0.8 to 0.67 [12].

Fig. 6: Oxygen tank. The dimensions are measured in [m]

The figure below (Fig. 7) represents an overview of the payload configuration.

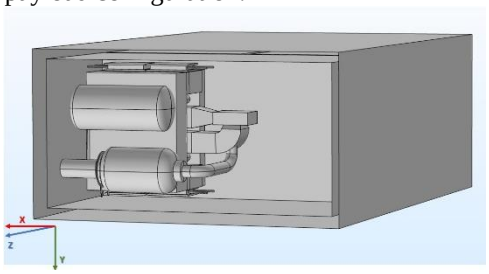

Fig. 7: Payload configuration

2.2. Thermal Management System

Considering the payload discussed in the previously section, some active thermal pieces of equipment are considered in order to maintain the operative temperature inside the test chamber:

- Heater
- Thermoelectric coolers or Peltier Cells
- Stirling Cryocooler

2.2.1. Heater

On small spacecraft, electrical resistance heaters are typically used to maintain battery temperature during cold cycles of the orbit and are controlled by a thermostat or temperature sensor.

Since the microorganisms have their own specified temperature maintenance requirement, the heater was used during the past CubeSat mission with a biological payload. NASA Ames biological nanosats (GeneSat, PharmaSat, O/OREOS, SporeSat, EcAMSat and Biosentinel) all utilize actively-controlled resistance heaters for precise temperature maintenance for their biological payloads with close-loop temperature feedback to maintain the biology temperatures. [16]

2.2.2. Thermoelectric coolers

The TECs are miniature solid-state heat pumps capable of providing localized cooling to devices that require cold temperature. TECs in space have become relatively common for star tracker and IR sensor. TECs provide cooling via the Peltier effect, which is the cooling that results from the passage of an electric current through a junction formed by dissimilar metal. When the TEC is switched on, heat is pumped from the cold junction to the hot junction.[21]

Regarding the past use of this component, the Argus-1000 instrument onboard of CanX-2 uses a programmable Peltier cooler to enhance the Signal-to-Noise Ratio (SNR) of their linear gallium arsenide CMOS detector [17].

2.2.3. Stirling Cryocooler

As the TECs, the Cryocooler is useful to control the temperature for instruments such as high precision IR sensors. The use of cryocoolers is associated with longer instrument lifetimes, low vibration, high thermodynamic efficiency, low mass and supply cooling temperatures less than 50 K.

In this study, a Stirling cryocooler is considered. It is a heat engine that operates by cyclic compression and expansion of air or other gas (working fluid) at different temperature. The thermodynamics cycle used by the cryocooler is the Stirling cycle that consists of four reversible thermodynamic processes involving pressure and volume changes. As can be seen in the Fig. 8, an ideal thermodynamic cycle made up of two isothermal and two isometric regenerative processes.[22]

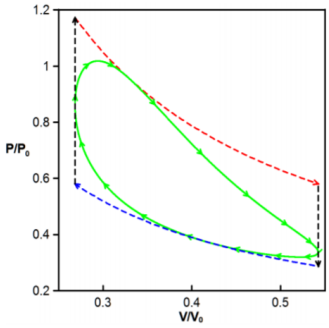

Fig. 8: Idealized Stirling cycle and real Styrling cycle (green line)[22]

As can be seen in the Fig. 9, a linear Stirling cooler is made up of two principal components: the Stirling Finger and a compressor. As described in the reference [23], initially, the pistons in the compressor are pushed towards each other, compressing the gas. In this stage, the compression is nearly isothermal, heat output being dissipated via heat sinks around the compressor and the base of the cold finger. In the next stage, the pistons remain stationary, but the displacer moves downwards as the gas above it compresses, and gas flows through the regenerator into the space inside the end of the cold finger, giving up heat as it passes through. During the third phase, which is nearly isothermal like this one, the pistons are driven outwards and the gas expands, drawing in heat from around the cold finger. In the fourth phase, the pistons again remain stationary but the displacer moves upwards under spring pressure because of the lower gas pressure in the expansion space. The gas takes up stored heat from the regenerator and re-enters the compression space at ambient temperature [23].

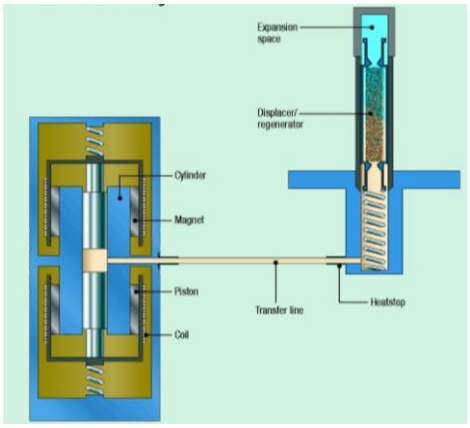

Fig. 9: Linear Stirling cooler[23]

Nowadays, the Technology Readiness Level (TRL) for this technology is 6-7 and, thanks of their small size and power, they can be used for small satellite application [16].

3 Methodology and theory.

3.1 Methodology overview

In order to design the TMS able to meet the environmental requirement for the payload, two kinds of analyses are performed:

- Radiative analysis to compute the heat fluxes in the orbit environment and, thus, the fluxes incoming to MoonBIO.
- Thermo fluid-dynamic analysis to compute the temperature and to analyse behaviour of the flow.

For the first one, in order to design the TMS in worst condition, two orbits are considered: hot and cold orbit.

Once obtained the heat fluxes, a steady state thermo fluid-dynamic analysis is performed for each part of the payload in order to compute the temperature in the sample chamber and the heat fluxes of the TCS needed to keep the operative temperature.

3.2 Thermal analysis: Radiative analysis

The principal forms of environmental heating on orbit are solar radiation, sunlight reflected off the planet (albedo), and IR energy emitted from the planet. The overall thermal control of a satellite on orbit is usually achieved by balancing the energy emitted by the spacecraft as IR radiation against the energy dissipated by its internal electrical components plus the energy absorbed from the environment. [21]

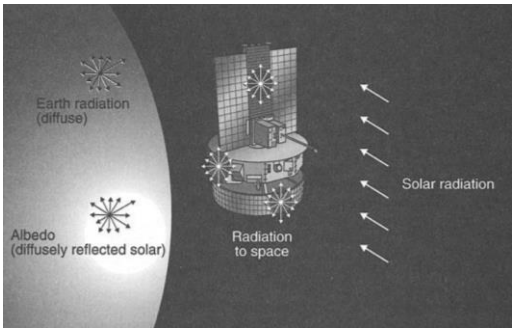

Fig. 10: Satellite thermal environment[21]

In order to design the TCS and to verify the temperature requirements, the thermal analysis shall be performed. The objective of all thermal analysis is to solve the following equation, named "general heat-transfer equation":

$$\rho C_p \frac{\partial T}{\partial t} = \nabla \cdot (K \cdot \nabla T) + Q(T,t) \quad (1)$$

where ρ is density (kg/m^3), C_p is specific heat (J/kg*°C), K is conductivity tensor (W/m*°C), T is temperature (°C), t is time (sec) and Q is the source term (W/m^3). In summary, the last term depends on all effects described before and summarized in the Fig. 10.

Thus, the heat fluxes from the space environment could be compute thanks the following equations:

$$q_s = \alpha S \quad (2)$$

$$q_A = a\alpha\rho S \quad (3)$$

$$q_{IR} = \varepsilon F_p C_{IR} \quad (4)$$

Where:

- q_s, q_A, q_{IR} are the heat flux caused by solar radiation, Albedo and IR of the planet fluxes [W/m^2]
- S is the Solar constant (mean value 1367 W/m^2)
- α and ε are the absorptivity and the emissivity of the material
- a and C_{IR} are the albedo and the IR constant
- F_p is the planet view factor

Inside the spacecraft, all components are heat sources and they emit thermal radiation. Therefore, the radiant flux for each source to a blackbody is governed by Stephan-Bolzman equation:

$$q_i(T,t) = F_{ij}\varepsilon_i\sigma T_i^4 \quad (5)$$

where σ is Stephan-Bolzman constant, F_{ij} is the view factor between a surface i and surface j and T_i is the temperature of the body i.

3.3 Thermo fluid-dynamic analysis

Using the heat fluxes computed thanks to radiative analysis, it is possible to measure the temperature of the fluid along of its path. The reference equations [24] are:

- Continuity equation (6)
- Momentum equation (7)
- Energy equation (8)

Thus, the equations in steady state are:

$$\nabla \cdot (\rho u) = 0 \quad (6)$$

$$\rho(u \cdot \nabla)u = -\nabla \mathrm{p} + \nabla \cdot \bar{\bar{\tau}} + \rho f \quad (7)$$

$$\rho \nabla \cdot (h\, u) = -(u \cdot \nabla)p + \nabla \cdot (K \nabla T) + (\bar{\bar{\tau}} \cdot \nabla)u \quad (8)$$

where

- ρ is density
- u is speed vector
- p is pressure
- $\bar{\bar{\tau}}$ is viscous stress tensor
- h is specific enthalpy

Considering that the maximum speed is 0.5 m/s and reference length of 0.8 cm, the Reynolds number results to be Re<2100, thus it is possible to simplify the computation admitting an assumption of laminar flow [25].

4. Results and Discussion

4.1. Radiative Analysis

For the radiative analysis, the evaluation of heat fluxes from space environment is computed with C&R Thermal Desktop®. The measured fluxes are used to evaluate the radiative exchanges between the internal surfaces of the payload, computed with COMSOL Multiphysics®.

4.1.1. Model

For this analysis, the model, described in the Fig. 1, has been simplified, as can be seen in the Fig. 11 and Fig. 12.

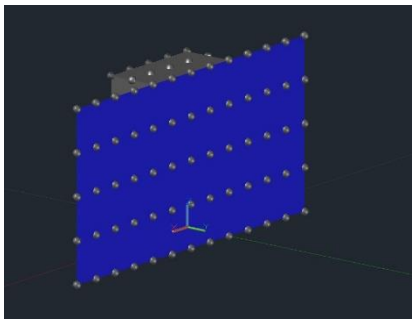

Fig. 11: External part the spacecraft

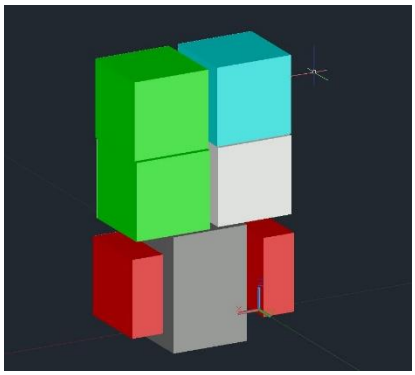

Fig. 12: Internal part of the spacecraft.

In the Fig. 12, the green bricks are the study domains that represent the biological payload for this analysis. For the hot and cold case, power dissipations for each component is summarized in the Table 2.

Table 2: Power dissipation

Component	Hot case	Cold case
Avionic (cyan)	4 W	4 W
Propulsion sys (grey)	11 W	4 W
Pack battery* (red)	3 W	0 W
MoonRAD	3 W	0 W

*heater

Regarding the material, during the preliminary analysis a state-of-the-art study is performed and the optical properties are reported in the Table 3.

Table 3: Optical properties for each component

Component	α	ε
Avionic (cyan)	0.88	0.49
Propulsion sys (grey)	0.70	0.1
Pack battery (red)	0.34	0.55
MoonRAD	0.1	0.17
Structure (grey external)	0.88	0.88
Solar cell (blue external)	0.650	0.85

The cold and hot orbits have the same orbital parameters mentioned in the Table 1. The only parameter that changes is the Right Ascension of the Ascending Node (RAAN). As can be seen in Fig. 13, with RAAN equal to 130 deg, it is possible to have an orbit in which the orbital period is equal to the daylight time (Hot

Orbit). As far as the cold orbit is concerned, an orbit with the RAAN equal to 25 deg is considered because it is a suitable compromise between high eclipse time and low fluxes incoming to the satellite during the daylight (Fig. 14).

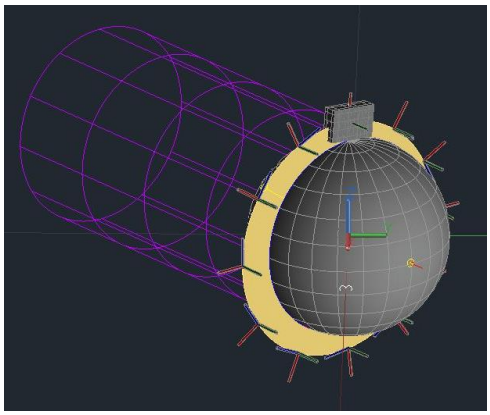

Fig. 13: Hot orbit with RAAN equal to 130 deg

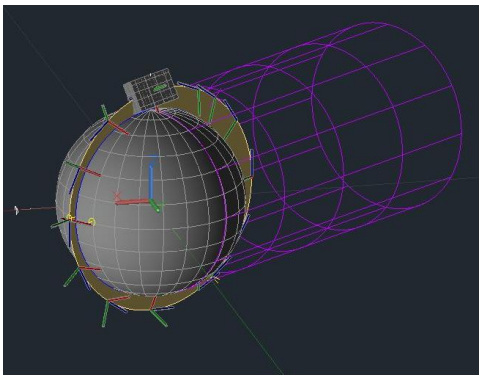

Fig. 14: Cold orbit with RAAN equal to 25 deg

Once the heat fluxes from the environment are measured, it is possible to evaluate the heat fluxes around the green bricks (Fig. 12). Thus, radiative analysis, considering the same domain, is conducted with COMSOL Multiphysics®, to analyse the internal radiative heat exchange between the shell of the satellite and equipment. As can be seen by the Fig. 15, the model used for the radiative analysis has been simplified with respect to the configuration described in the section 2.1.

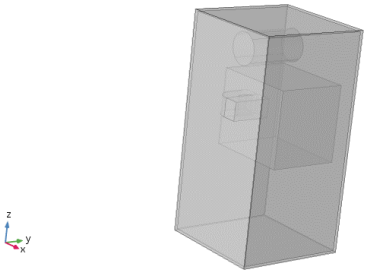

Fig. 15: Model for radiative analysis (COMSOL Multiphysics®)

4.1.2. Hot Case

The simulation time is set to 10 orbits and the results are summarized in the Fig. 16. As it can be seen from the graph, the trends of the heat fluxes fluctuate around a constant value.

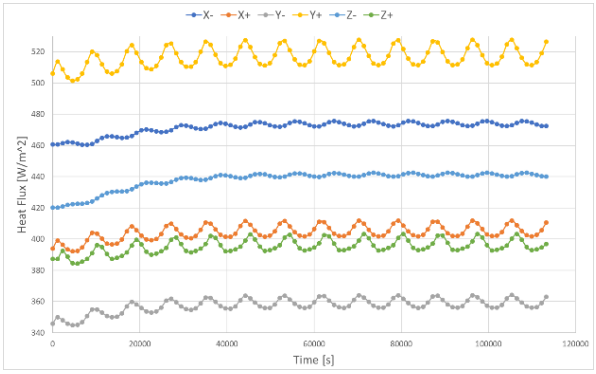

Fig. 16: Hot orbit fluxes from space environment

These fluxes are applicated in the walls of the model in Fig. 15. and as results, it is possible to obtain the incoming fluxes for each component (Fig. 17).

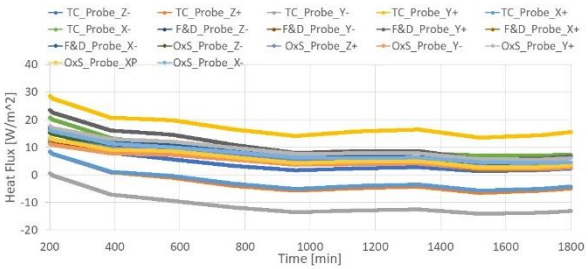

Fig. 17: Hot case fluxes incoming to the payload

4.1.3. Cold Case

As in the hot case, 10 orbits are simulated, and the results are reported in the Fig. 18 and Fig. 19.

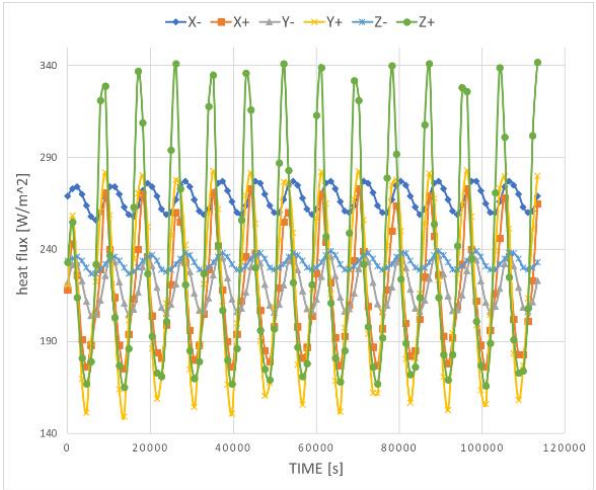

Fig. 18: Cold orbit fluxes from space environment

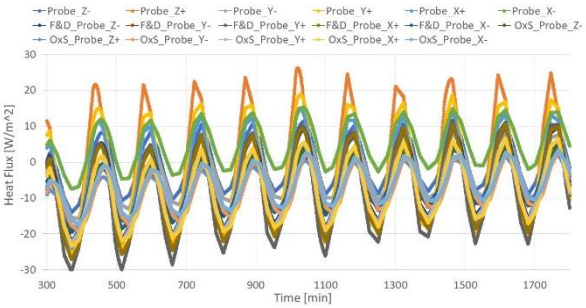

Fig. 19: Cold case fluxes

The fluctuation of the trend is more relevant with respect to the hot case. Thus, since in this study a steady state simulation is done, the lowest heat fluxes for each component are considered for the other analysis.

4.2. Thermo fluid-dynamic analysis

For this analysis, the temperature of the flow and the heat fluxes needed to keep the operative temperature are computed with COMSOL Multiphysics®.

4.2.1. Model

The Thermo fluid-dynamic analysis is performed for each component of the payload described in the section 2.1. Simple models are also used for this study and 5 different flow speeds are simulated both for cold case and for hot case. To considerer a worst cold and hot case, an environmental temperature of 50°C (for the hot case) and -10°C (for the cold case) is considered. Starting from the sample chamber, the inlet temperature of the flow is 30°C and with this analysis it is possible to obtain the temperature of the outlet section for each component of the payload.

For this preliminary analysis, it is supposed that the thermal control takes place on the *inlet plenum (*i.e before the flow reaches the sample chamber*).* In addition, the temperature must be controlled in the tank in order to decrease the difference temperature between the tank and test chamber.

4.2.2. Hot Case

The firsts analysed items are the Sample Chambers, applying the radiative heat fluxes to the surfaces computed in the previously analyses and reported in Fig. 17. As can be seen by the graph of the lateral sample (Fig. 20), it is possible to obtain a tolerance of 5°C with 0.1 m/s. For the middle sample, a lower tolerance is reached for each flow speed because it is less influenced by lateral fluxes.

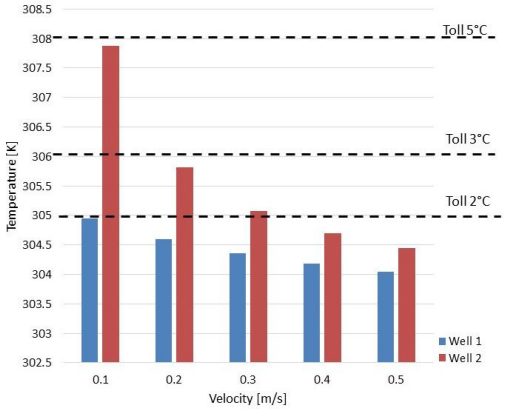

Fig. 20: Lateral sample chambers.

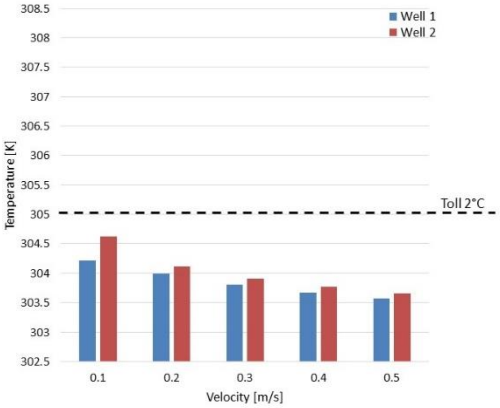

Fig. 21: Middle Sample chamber

While increasing the flow speed, the difference temperature between the two bacterial wells (the *well 1* is near the *inlet section* and the *well 2* is near the *outlet section)* decreases. This effect can be seen in the Fig. 22, Fig. 23, Fig. 24.; the distribution of the temperature on the plane becomes more uniform by increasing of the flow speed.

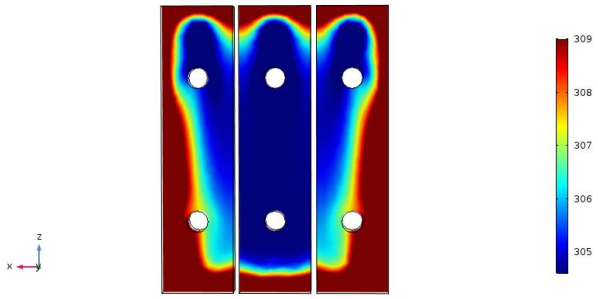

Fig. 22: Temperature [K] for flow speed equal to 0.1 m/s (middle section).

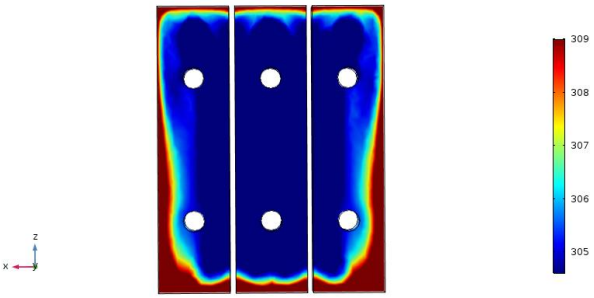

Fig. 23: Temperature [K] for flow speed equal to 0.3 m/s (middle section)

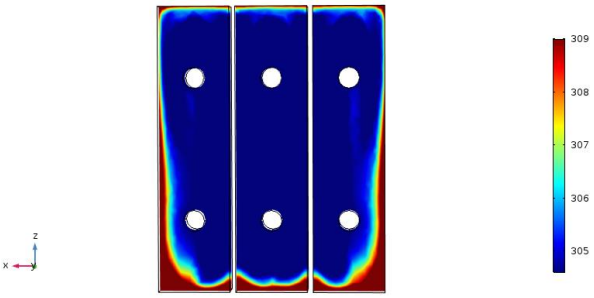

Fig. 24: Temperature [K] for flow speed equal to 0.5 m/s (middle section)

After the sample channel, the flow passes the *outlet plenum* and *the pipe-line* and it reaches the following temperature.

Table 4: Temperature in the outlet section for *Outlet plenum* and *Pipe-line*

Speed [m/s]	Outlet plenum [K]	Pipe-line [K]
0.1	314.47	321.68
0.2	311.49	318.54
0.3	309.83	316.15
0.4	308.75	314.39
0.5	307.98	313.04

Then, the flow reaches the *inlet plenum* and here it is subject to the heat fluxes from TCS. The cooling power is iterated in order to reach the reference temperature of 30°C and the values computed is used for the preliminary design of the TCS. The results are reported in the following table.

Table 5: Heat fluxes for TCS and temperature in outlet section of the *inlet plenum*

Speed [m/s]	Temperature [K]	Heat flux [W/m^2]
0.1	304.14	-300
0.2	302.47	-500
0.3	304.96	-500
0.4	304.01	-600
0.5	303.11	-700

As can be seen by the Table 5, with increasing the flow speed, the absolute value of the heat flux increases, making the temperature control more demanding in terms of energy.

As you can see in the figure below (Fig. 25), considering the flow speed equal to 0 m/s and the pressure of 10 atm, with 0.450 W of cooling power, it is possible to keep the operative temperature for the tank.

Fig. 25: Temperature distribution [K] in the Oxygen tank with 0.450 W.

4.2.3. Cold Case

As in the hot case, the flow in the Sample Chambers is analysed, applying the radiative heat fluxes to the surfaces computed in the previously analyses and reported in Fig. 19. Here again, the tolerance of 10°C is meet too and, by increasing the flow speed, the difference of the temperature between of the wells decreases with increasing of the flow speed (Fig. 26, Fig. 27).

Regarding the distribution of the temperature on the plane, it become uniform with increasing of the flow speed.

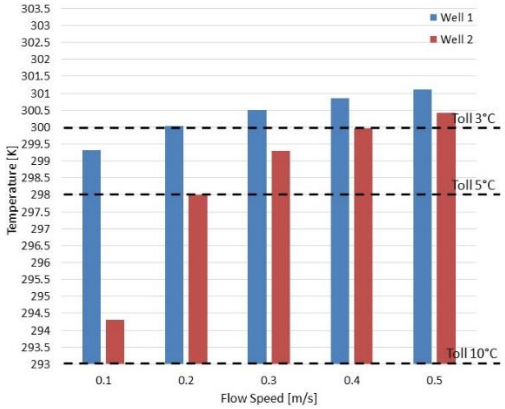

Fig. 26: Temperature trend [K] on lateral sample chamber

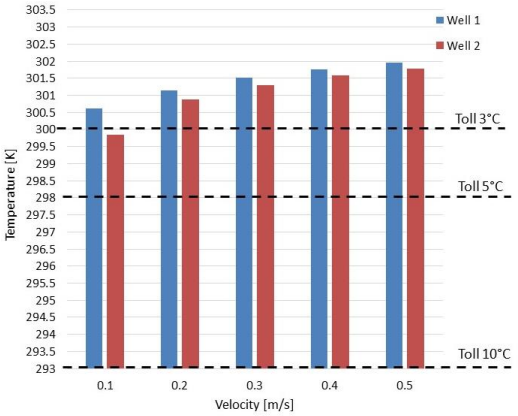

Fig. 27: Temperature trend [K] on middle sample chamber

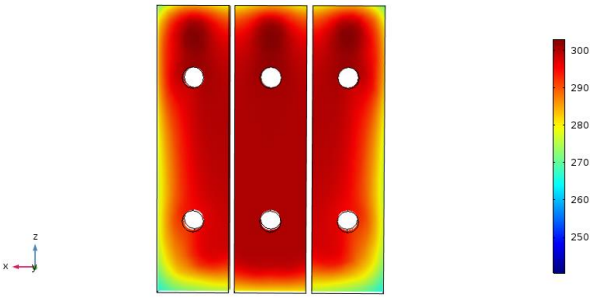

Fig. 28: Temperature [K] for flow speed equal to 0.1 m/s (middle section)

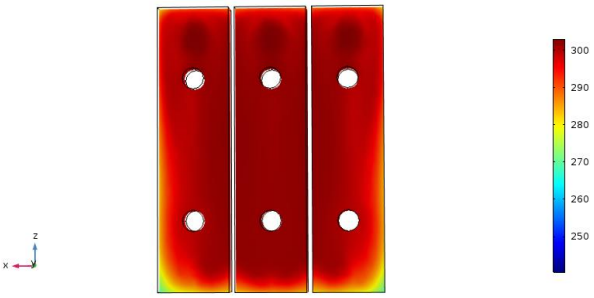

Fig. 29:Temperature [K] for flow speed equal to 0.3 m/s (middle section)

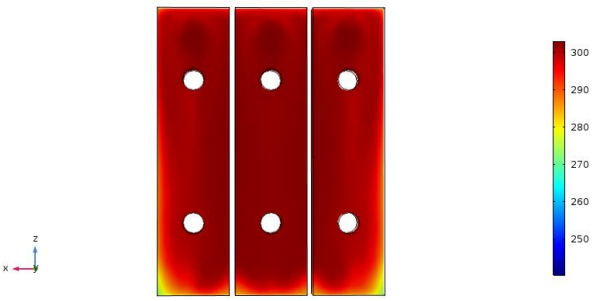

Fig. 30: Temperature [K] for flow speed equal to 0.5 m/s (middle section)

The temperatures in the outlet section of *outlet plenum* and *pipe-line* are reported in the Table 6.

Table 6: Temperature in the outlet section for *Outlet plenum* and *Pipe-line*

Speed [m/s]	Outlet plenum [K]	Pipe-line [K]
0.1	281.80	266.52
0.2	287.70	274.61
0.3	290.88	279.70
0.4	292.92	283.20
0.5	294.35	285.76

In the *inlet plenum*, the heat fluxes required to maintain 30°C in the outlet section are reported in the following table Table 7.

Table 7: Heat fluxes for TCS and temperature in outlet section of the *inlet plenum*

Speed [m/s]	Temperature [K]	Heat flux [W/m^2]
0.1	304.36	800
0.2	299.99	1000
0.3	300.00	1000
0.4	301.51	1200
0.5	300.91	1200

For the tank, the same condition of the hot case is considered, and the operative temperature is reached with 0.8 W of power dissipation.

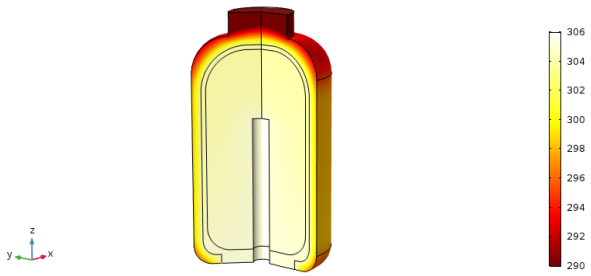

Fig. 31: Temperature distribution [K] in the Oxygen tank with 0.8 W.

4.3. Preliminary TCS configuration

Thanks to the results of the previous analyses, it is possible to preliminarily design the TCS configuration. As discussed in the section 4.1.1, the temperature of the oxygen is controlled on the *inlet plenum* and in the tank. For the *inlet plenum*, it is possible to consider one heater and one TEC on a metal foil in order to uniform the flux all over the top surface of the plenum (Fig. 32).

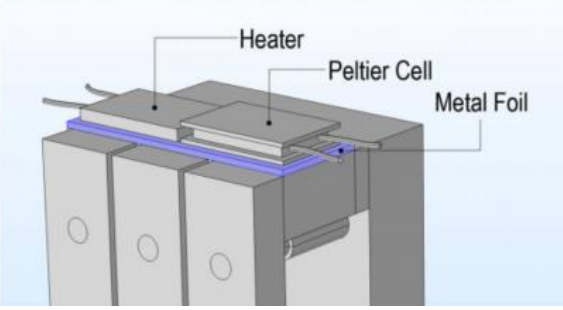

Fig. 32: Heat and TEC on the inlet plenum

Regarding the hot case, the maximum computed heat flux is -700 W/m^2. Considering that the sizes of metal foil are 60 x 20 mm^2, the cooling power results to be 0.84 W. For the cold case, the maximum heat flux results to be 1200 W/m^2 and the power results to be 1.44 W. Among COTS components, for the Peltier cells is considered one of Custom Thermoelectric [26] with the size compliant with this case study (Fig. 33). From the datasheet, it is possible to measure the power consumption for 0.84 W of cooling power and the value results to be 0.975 W. In this preliminary analysis, as concern the Margin of philosophy of ESA [27], 20% of margin is adopted, thus the power consumption for the peltier cells results to be about 1.2 W.

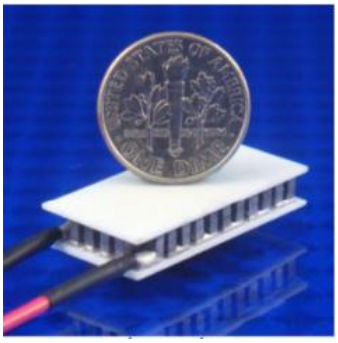

Fig. 33: Custom Thermoelectric model 04711-5L31-04CGL [26]

The same process is performed with the cold case and, thus, a possible heater could be a COTS one of PTI Pelonis Technologies [28] with a power consumption of 2.01 W.

Fig. 34:PTI Pelonis Technologies heater (model TSA0200032aR1.12) [28]

For the tank, circular heater and Stirling cryocooler are used and the configuration is described in the following figure (Fig. 35)

.

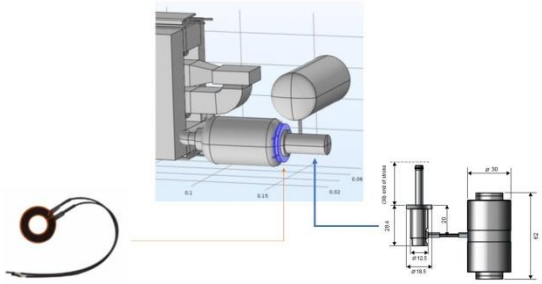

Fig. 35: TCS configuration for the tank

Here again, the heater is a COTS one of PTI Pelonis Technologies[29] with a power consumption of 1.42 W. Regarding the Stirling cryocooler, the Thales Cryogenics UP 8197 is chosen and the sizes are reported in the following figure (Fig. 36).

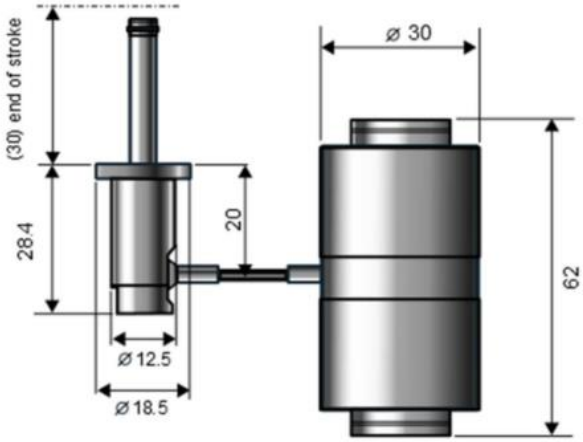

Fig. 36: Thales Cryogenics UP 8197. Dimensions in [mm] [30]

Since the actual cooling power is low with respect to its nominal mode (1.5 W of cooling power in order to reach 150K from 293K, demanding 15W of energy) [30], in order to measure the power consumption, a linear relation between the maximum power consumption to deference temperature between environmental and Stirling finger is considered [31]. Thus, to reach 30°C from 50°C, for a cooling power of 0.45 W, the power consumption results to be about 1.8W (with 20% of margin).

Thus, the power dissipation for each component is compliant with the power capability of the small satellite.

However, transient analysis is request, in order to evaluate the duty cycle useful for a detail power budget.

5. Conclusions

The study presented in this paper represents the first stage of a research on going at Politecnico di Torino aimed at increasing CubeSat capabilities and technologies in several domains. Advanced CubeSat missions might require thermal performance not attainable with current state of the art technology.

For example, it is expected that CubeSats with propulsion system will be critical from the thermal perspective, as shown in [32].

As result, it is possible to confirm that, with the chosen TCS, the temperature requirement is verified during the mission. After the analysis, it is possible to design a first configuration for the TCS and a possible operating mode to heat or cool the oxygen flow.

The flow could be heated or cooled with low speed of flow and, after, the temperature of the sample chamber could be uniformed increasing the flow speed.

However, for a detail power budget, a transient analysis must be performed. In addition, an optimal configuration of the TCS could be found considering heating or cooling the flow also in the *outlet plenum* or considering the surface finishes and insulation.

The Stirling cooler chosen is not an optimal solution, but in this study, the authors want to present a possible application of it. Indeed, this TCS could use for biological experiment that request thermal requirement more stringent (e.g cryobiological experiment).

Acknowledgements

Authors wants to acknowledge all student of the CubeSat @PoliTo Team, in particular Giorgio Ammirante and Sergio Zanola for the great support during the writing of the paper.

References

[1] NASA, The Global Exploration Roadmap What is New in The Global Exploration Roadmap, (2018). https://www.globalspaceexploration.org/wordpress/wp-content/isecg/GER_2018_small_mobile.pdf.

[2] D. Masutti, A. Denis, T. Berger, F. Nichele, S. Corpino, L. Franchi, M. Cardi, G. Martinotti, E. Rabbow, A CUBESAT FOR THE ANALYSIS OF THE LUNAR RADIATION ENVIRONMENT: THE MOONCARE MISSION, in: 4S Syphosium 2018, 2018: pp. 1–15.

[3] C.N.A. Schwadron, T. Baker, B. Blake, Lunar Radiation Environment and Space Weathering from the Cosmic Ray, J. Geophys. Res. 117 (2012). doi:10.1029/2011JE003978.

[4] J. Goswami, M. Annadurai, Chandrayaan-1: India's first planetary science mission to the Moon, 2009.

[5] G. Obiols-Rabasa, S. Corpino, R. Mozzillo, F. Stesina, Lessons learned of a systematic approach for the E-ST@R-II CUBESAT environmental test campaign, in: Proc. Int. Astronaut. Congr. IAC, 2015: pp. 8474–8482.

[6] D. Masutti, A. Denis, R. Wicks, J. Thoemel, D. Kataria, A. Smith, J. Muylaert, The QB50 mission for the investigation of the mid-lower thermosphere: Preliminary results and lessons learned, in: Proc. Int. Astronaut. Congr. IAC, 2017: pp. 5785–5796.

[7] S. Corpino, G. Obiols-Rabasa, R. Mozzillo, F. Nichele, E-st@r-I experience: Valuable knowledge for improving the e-st@r-II design, Acta Astronaut. 121 (2016) 13–22. doi:10.1016/j.actaastro.2015.12.027.

[8] A. Denis, J. Pisane, OUFTI-1, the educative nanosatellite of the University of Liége, Belgium, in: 60th Int. Astronaut. Congr. 2009, IAC 2009, 2009: pp. 8312–8314.

[9] L. Feruglio, S. Corpino, Neural networks to increase the autonomy of interplanetary nanosatellite missions, Rob. Auton. Syst. 93 (2017) 52–60. doi:10.1016/j.robot.2017.04.005.

[10] R. Staehle, D. Blaney, H. Hemmati, Interplanetary CubeSats: Opening the Solar System to a Broad Community at Lower Cost, J. Small Satell. 2 (2013) 161–186. http://jossonline.com/downloads/0201 Interplanetary CubeSats Opening the Solar System to a Broad Community at Lower Cost.pdf.

[11] R. Walker, D. Koschny, C. Bramanti, E.S.A. Cdf, Miniaturised Asteroid Remote Geophysical Observer (M-ARGO): A Stand-alone Deep Space CubeSat System for Low- cost Science and Exploration Missions, 6th Interplanet. CubeSat Work. (2017).

[12] S. Clark, NASA confirms first flight of Space Launch System will slip to 2019 – Spaceflight

Now, 2017-04-28. (n.d.). https://spaceflightnow.com/2017/04/28/nasa-confirms-first-flight-of-space-launch-system-will-slip-to-2019/ (accessed September 12, 2018).

[13] J. Schoolcraft, A.T. Klesh, T. Werne, MarCO: Interplanetary Mission Development On a CubeSat Scale, SpaceOps 2016 Conf. (2016) 1–8. doi:10.2514/6.2016-2491.

[14] J. Pezent, R. Sood, A. Heaton, Near Earth Asteroid (NEA) Scout Solar Sail Contingency Trajectory Design and Analysis, 2018. doi:10.2514/6.2018-0199.

[15] S. Corpino, M. Caldera, F. Nichele, M. Masoero, N. Viola, Thermal design and analysis of a nanosatellite in low earth orbit, Acta Astronaut. 115 (2015) 247–261. doi:10.1016/j.actaastro.2015.05.012.

[16] B. NASA Yost, 07. Thermal Control – State of the Art of Small Spacecraft Technology, (2018). https://sst-soa.arc.nasa.gov/07-thermal (accessed September 9, 2018).

[17] D. Selva, D. Krejci, A survey and assessment of the capabilities of Cubesats for Earth observation, Acta Astronaut. 74 (2012) 50–68. doi:10.1016/j.actaastro.2011.12.014.

[18] J. Berg, CryoCube-1 : A Cryogenic Fluid Management CubeSat CryoCube Project Intro, (2018) 1–10.

[19] R. Walker, J. Vennekens, R. Fisackerly, J. Carpenter, I. Carnelli, M. Fontaine, LUnar CubeSats for Exploration (LUCE) mission concept studies General SysNova objectives, (2017).

[20] G. Minelli, A. Ricco, C. Beasley, J. Hines, E. Agasid, B. Yost, D. Squires, C. Friedericks, M. Piccini, G. Defouw, M. Mcintyre, R. Ricks, M. Parra, M. Diaz-Aguado, L. Timucin, M. Henschke, M. Lera, M. Tan, M. Cohen, L. Bica, O/OREOS Nanosatellite: A Multi-Payload Technology Demonstration, 2010.

[21] D.G. Gilmore, Spacecraft Thermal Control Handbook Volume I : Fundamental Technologies, Second edi, California, 2002.

[22] A. Romanelli, Alternative thermodynamic cycle for the Stirling machine, (2017) 1–14. doi:10.1119/1.5007063.

[23] EUREKA, Keeping cool with new technologies, (2004). http://www.shelleys.demon.co.uk/fnov04fr.htm.

[24] A.K. Hoffmann, Computational fluid dynamics. Volume 1, (2001).

[25] F.D. Young, R.M. Munson, A Brief introduction to FLUID MECHANICS, fifth edit, 2011.

[26] CUSTOM THERMOELECTRIC, TEC Specification Sheet Part : CUSTOM THERMOELECTRIC model 04711-5L31-04CGL, (2010).

[27] SRE-PA & D-TEC staff, Margin philosophy for science assessment studies, 2012.

[28] Pelonis Technologies, Model Number TSA0200032aR1.12, 0.31 Watt per Centimeter Square (W/cm^2) Power Density and 1.34 Ampere (A) Current Ultra-Thin Flexible Heater On Pelonis Technologies, Inc., (n.d.). https://catalog.pelonistechnologies.com/item/low-voltage-1-5-24v-rectangular-ultra-thin-flexibl/rectangular-1-5-v-ultra-thin-flexible-heaters/tsa0200032ar1-12 (accessed September 13, 2018).

[29] PTI Pelonis Technologies Model Number TSA025d006aR1.58, (n.d.). http://catalog.pelonistechnologies.com/item/category-3001493/round-1-5-volt-ultra-thin-flexible-heaters/tsa025d006ar1-58 (accessed September 13, 2018).

[30] Thales, Thales UP 8197 1500 mW @ 150 K / SWaP ¼" IDCA (short) - Thales Cryogenics, (n.d.). http://www.thales-cryogenics.com/products/coolers/up-ls/up8197/ (accessed September 14, 2018).

[31] J. Raab, E. Tward, Small Space Cryocoolers, (2011) 1–8. http://arc.aiaa.org/doi/pdf/10.2514/6.2011-805%5Cnpapers3://publication/uuid/AF5AB5D5-8FD0-4BB3-8B2F-734F9FCD64C8.

[32] F. Stesina, S. Corpino, G. Saccoccia, G. Del Amo J.A, E. Bosch Borràs, Design of a test platform for miniaturized electric propulsion system, in: IAC 2018, Bremen, 2018.